Loss of tight junction integrity abolishes the epithelial phenotype: the case of Claudin11deficiency in testis.

Séverine Mazaud-Guittot, Emmanuelle Meugnier, Sandra Pesenti, X. Wu, Hubert Vidal, A Gow, Brigitte Le Magueresse-Battistoni

Loss of tight junction integrity abolishes the epithelial phenotype: the case of Claudin11 deficiency in testis.

Running title: Claudin11 and loss of the Sertoli cell epithelial phenotype

Mazaud-Guittot S.[1,2,3,4,5,9,10], Meugnier E.[1,2,3,4,5], Pesenti S.[1,2,3,4,5], Wu X.[6], Vidal H[1,2,3,4,5], Gow A.[6,7,8], Le Magueresse-Battistoni B.[1,2,3,4,5]

Address :
[1]Inserm, U870, Oullins, France; [2]INRA, UMR1235, Oullins, France; [3]INSA-Lyon, RMND, Villeurbanne, France; [4]Université Lyon 1, Lyon, France; [5]Hospices Civils de Lyon, Lyon, France.

[6]Center for Molecular Medicine and Genetics, [7]Karman and Ann Adams Department of Pediatrics, [8]Department of Neurology, Wayne State University, 3217 Scott Hall, 540 E Canfield, Detroit, MI, U.S.A.

Present address : [9] Inserm, U625, Rennes, France ; [10] Univ Rennes I, Campus de Beaulieu, IFR-140, GERHM, Rennes, F-35042, France.

Corresponding authors : Brigitte Le Magueresse-Battistoni at Brigitte.lemagueresse@inserm.fr and Séverine Mazaud-Guittot at severinemazaud@yahoo.fr

ABSTRACT

Tissue integrity relies on barriers formed between epithelial cells. In the testis, the barrier is formed at the initiation of puberty by a tight junction complex between adjacent Sertoli cells, thereby defining an adluminal compartment where meiosis and spermiogenesis occur. Claudin11 is an obligatory protein for tight junction formation and barrier integrity in the testis. It is expressed by Sertoli cells, and spermatogenesis does not proceed beyond meiosis in its absence, resulting in male sterility. Sertoli cell maturation – arrest of proliferation and expression of proteins to support germ cell development – is known to parallel tight junction assembly; however, the pathophysiology underlying the loss of tight junctions in the mature testis remains largely undefined. Herein, we use immunohistochemistry and microarrays in wild-type and *Claudin11*$^{-/-}$ testes from mice to demonstrate that adult *Claudin11*$^{-/-}$ Sertoli cells re-enter the cell cycle while maintaining expression of several differentiation markers. Dividing Sertoli cells lose polarity, detach from the basement membrane and are eliminated through the lumen together with apoptotic germ cells that they have phagocytosed. Thus, *Claudin11*$^{-/-}$ Sertoli cells exhibit a unique phenotype whereby loss of tight junction integrity results in loss of the epithelial phenotype but not the progression to a tumorigenic phenotype.

INTRODUCTION

The integrity of epithelial cell layers is maintained by intercellular junctional complexes composed of adhesive (adherens junction, desmosomes, hemidesmosomes) and occluding (tight) junctions, and gap junctions promote intercellular communication. The transmembrane proteins constituting these junctions are linked to components of the actin and

intermediate filament cytoskeletons, and a growing number of cytoplasmic scaffolding molecules associated with these junctions are involved in regulating such diverse processes as transcription, cell proliferation, cell polarity and the assembly of regulated diffusion barriers. Typically, tight junctions (TJs) define the boundary between the apical and basolateral domains of epithelial cell membranes and function as the primary barrier to diffusion of macromolecules, ions, and small non-charged solutes through the paracellular pathway (22, 47).

Most blood-tissue barriers, such as the blood-brain and blood-retinal barriers, are generated by endothelial cell TJs in specialized microvessels. By contrast, the blood-testis barrier (BTB) is generated and maintained by Sertoli cells in the seminiferous epithelium and is physically remote from microvessels of the interstitium. The BTB is also unique because it is cyclically restructured during spermatogenesis when preleptotene spermatocytes migrate into the adluminal compartment and enter meiosis. Thus, the BTB divides the seminiferous epithelium into two compartments: the basal compartment, which forms the niche for spermatogonia proliferation and renewal, and the adluminal compartment, where meiosis and spermiogenesis occur.

Both the structural integrity of the seminiferous epithelium and the BTB are maintained by the highly specialized actin filament network of the Sertoli cell cytoskeleton, known as the ectoplasmic specialization (ES). Ectoplasmic specializations are complex cytoskeletal structures occurring in submembranous regions adjacent to TJs (BTB) and the apical adhesion sites of spermatogenic cells (14, 15, 38, 43). They consist of bundles of actin filaments sandwiched between the plasma membrane and cisternae of the endoplasmic reticulum (7, 14, 15, 38, 43). Because they are closely associated with junctional sites, ESs are thought to play a major role in maintaining and regulating intercellular junction assembly (14, 34, 42, 44, 58-60, 62).

The molecular composition of the BTB has been the subject of numerous studies reviewed in (32) and Sertoli cell TJs are composed, at least, of the transmembrane proteins claudin 11, claudin 3, occludin, junction associated molecule (JAM-A) and the coxsackie virus and adenovirus receptor (CAR) (32, 36). The phenotypes of mice deficient in various components of these TJs varies from normal (no apparent phenotype) as revealed in *JAM-A*$^{-/-}$ mice (12), to slowly degenerative as for *Occludin*$^{-/-}$ mice (45), to sterility in *Claudin11*$^{-/-}$ mice (21). *Claudin11*$^{-/-}$ mice exhibit neurologic, auditory and reproductive deficits, including slowed central nervous system (CNS) nerve conduction, conspicuous hind limb weakness, profound sensorineural deafness and male sterility (13, 20, 21).

In the testis of *Claudin11*$^{-/-}$ mice, spermatogenesis does not proceed beyond the spermatocyte stage and cell clusters are observed in the seminiferous lumen. To understand the relationship between claudin11 loss and seminiferous tube disorganization, we have determined the aetiology of this phenotype, in particular during the formation of the BTB. Our comprehensive survey reveals that in the absence of claudin11, Sertoli cells do not form a mature BTB which induces a spermatogenesis defect in neighbouring germ cells. Furthermore, Sertoli cells lose polarity, detach from the basement membrane, undergo an epithelial-to-fibroblastic cell shape transformation and re-enter the cell cycle while maintaining expression of differentiation markers. These changes are associated with TJ regulation as well as actin-related and cell cycle gene expression. Thus, *Claudin11*$^{-/-}$ Sertoli cells exhibit a unique phenotype in that the loss of TJ integrity induces the loss of an epithelial phenotype which does not progress toward a tumorigenic phenotype.

MATERIAL AND METHODS

Animal handling, tissue collection and processing

Males were injected intraperitoneally with 50 mg/kg bromodeoxyuridine (BrdU) dissolved in saline 3 h before sacrifice. Testes and epididymides collected at P7, P10, P13, P15, P20, P28, P60, P90 and P180 were either frozen on dry ice and stored at -80°C until processing for RNA analysis or processed for morphological studies. For histological and immunohistochemical analyses, tissues were fixed either in Bouin fixative or in 4% paraformaldehyde-PBS (pH 7.2) for at least 24 h, dehydrated in a graded series of ethanol, and paraffin-embedded using standard protocols. Five µm-thick sections were stained with the periodic acid-Schiff-haematoxylin technique (PAS).

Immunohistochemistry

Paraffin embedded tissues were deparaffinized in xylene and rehydrated in graded ethanol solutions and endogenous peroxidase activity was blocked with 0.3% hydrogen peroxide in methanol for 30 minutes. For all but claudin11 immunodetection, sections were boiled for 5 minutes in 0.1M citrate buffer (pH 6.0) for antigen retrieval, blocked with 10% horse serum (in PBS with 8% BSA) for at least 20 minutes, and finally incubated overnight at 4°C with primary antibody diluted in blocking solution (Dako Corp., Trappes, France). Primary antibodies were directed against claudin11 (diluted 1/100; Santa Cruz Biotechnologies Inc., Santa Cruz, CA), DDX4 (diluted 1/750; kindly provided by Dr. T. Noce), Clgn (TRA-369 antibody; diluted 1/1000; kindly provided by Dr. H. Tanaka), Gata4 (diluted 1/100; Santa Cruz Biotechnologies), phosphorylated serine 10 (ser10) of histone H3 (diluted 1/500; Upstate Biotechnology, Euromedex, Mundolsheim, France), BrdU (diluted 1/100; Roche), Vimentin (LN-6 clone; diluted 1/100; DakoCytomation, Trappes, France).

After washing in PBS, and depending on the primary antibody used, sections were incubated for 2 h with either horseradish peroxidase-conjugated anti-rabbit antibody (Envision™+ system-HRP, Dako Corp.), biotinylated anti-goat antibody (1/500 dilution; Vector Laboratories Canada, Burlington, Canada), anti-rat antibody (1/200 dilution; Vector Laboratories) and finally 30 minutes with a peroxidase-conjugated streptavidin-horseradish complex (LSAB®+ Kit, Dako Corp.). The reaction product was developed using 3,3'-diaminobenzidine tetrahydrochloride (DAB) (Sigma-Aldrich). Sections were counterstained with hematoxylin and mounted with Eukitt (Sigma-Aldrich). For negative controls, primary antibody was omitted. Slides were analyzed with Zeiss Akioskop II and Axiophot microscopes (Carl Zeiss, New York, NY) connected to a digital camera (Spot RT Slider, Diagnostic Instruments, Sterling Heights, MI).

For double immunolabeling, paraffin sections were prepared as above, incubated overnight with anti-Gata4 antibody (diluted 1/100), followed by sequential incubations with anti-goat Ig-Alexa Fluor 546 secondary antibody (1/1000; Invitrogen) 2 h at room temperature, anti-BrdU antibody (1/100), and anti-mouse Ig-Alexa Fluor 488 secondary antibody (1/1000; Invitrogen). Fluorochrome-labeled sections were mounted in Vectashield containing DAPI for nuclei visualization (Vector Laboratories Canada, Burlington, Canada). Slides were analyzed with a Zeiss Akiovert epifluorescence microscope (Carl Zeiss, New York, NY) connected to a digital camera (Spot RT Slider, Diagnostic Instruments, Sterling Heights, MI).

Terminal deoxynucleotidyltransferase-mediated dUTP-FITC nick end labeling (TUNEL) assays.

Detection of apoptotic cells was performed on paraffin sections using in situ cell death detection kit (Roche). After rehydratation, sections were boiled for 5 minutes in 0.1M citrate buffer (pH 6.0), and incubated for 1 h at 37°C with the TUNEL reaction mixture containing terminal transferase to label free 3′-hydroxy ends of genomic DNA with fluorescein-labeled deoxy-UTP. After washing, sections were incubated overnight at 4°C with Peroxidase converter (Roche). Apoptotic cells were revealed with DAB, and sections counterstained with hematoxylin.

Morphometric analysis

Apoptotic cells and germ cells in the division phases were quantified in transverse seminiferous tube sections stained for TUNEL and phosphorylated histone H3, respectively. For each animal, at least three non-serial testicular sections were used, and in each section, all transverse sectioned tubes were quantified, for a total of at least 100 tubes per animal (with a mean of 330 and 300 tubes). In addition, the number of phosphorylated histone H3 labelled cells was counted in at least 50 tubes per animal. Sertoli cell nuclei were quantified in transverse seminiferous tube sections stained for Gata4. For each animal, at least three non-serial testicular sections were used, and in each section, all transverse section tubes were quantified, for a total of at least 50 tubes per animal.

Microarray analysis

Total RNA was prepared from P20-old testes by using RNeasy minikit (Qiagen, Courtaboeuf, France). RNA integrity was determined with the Agilent 2100 Bioanalyzer and RNA 6000 Nano Kit (Agilent Technologies,Massy, France). A pool of P20 *Claudin11*$^{+/-}$ testes was used as a common reference. One microgram of total RNA was amplified with the Amino Allyl MessageAmp II aRNA kit (Ambion, Austin, TX) according to the manufacturer's instructions.

Fluorescent probes were synthesized by chemical coupling of 5 µg of aminoallyl aRNA with cyanine (Cy)3 or Cy5 dyes (GE Healthcare Biosciences, Orsay, France). After purification with an RNeasy Mini Kit (Qiagen, Courtaboeuf, France), probes were fragmented with 25X RNA Fragmentation Reagents (Agilent Technologies) and hybridized with 2X Agilent Hybridization Buffer (Agilent Technologies) to Mouse opArray (Operon Biotechnologies GmbH, Cologne, Germany) in an Agilent oven at 67°C for 16 h, following a dye swap experimental procedure. Microarrays were washed and scanned with a Genepix 4000B scanner (Axon Instruments, Foster City, CA).

TIFF images were analyzed using Genepix Pro 6.0 software (Axon Instruments). Signal intensities were log-transformed and normalization was performed by the intensity dependent Lowess method. To compare results from the different experiments, data from each slide were normalized in log-space to have a mean of zero using Cluster 3.0 software. Data were analyzed using the Significance Analysis of Microarray (SAM) procedure (55). Microarray data are available in the GEO database under the number GSE15492. Further analysis of GO and KEGG pathway enrichments were performed using the WebGestalt analysis toolkit (http://bioinfo.vanderbilt.edu/webgestalt/) (67).

Quantitative PCR

First-strand cDNAs were synthesized from 1 µg of total RNA in the presence of 100 U of Superscript II (Invitrogen, Eragny, France) and a mixture of random hexamers and

oligo(dT) primers (Promega, Charbonnières, France). Real-time PCR assays were performed with a Rotor-Gene™ 6000 (Corbett Research, Mortlake, Australia). PCR primers are listed in Table 1.

Data analysis

Statistical analyses were performed using the SigmaStat 2.0 software package. For cell counts, a One-way ANOVA followed by the appropriate post-hoc test was used to compare differences between groups, as specified in each figure legend. Significance was accepted at a confidence level of $p \leq 0.05$.

RESULTS

Chronology of the *Claudin11*$^{-/-}$ phenotype

To characterize the beginning of the testicular phenotype in *Claudin11*$^{-/-}$ mice, we first analyzed testis histological sections throughout postnatal testicular development (Fig. 1). At two weeks of age, seminiferous tubes contain Sertoli cells and early pachytene spermatocytes, which are the most mature cells of the germ cell lineage. One week later, early spermatids largely populate the tubes, and differentiating elongated spermatids are first detected at P28. At P60, when the animals are adults, spermatogenesis is cyclic and can be divided into 12 stages (I-XII) based on the morphological transformation of spermatids into spermatozoa in a process referred as spermiogenesis (39).

The first signs of disorganization in *Claudin11*$^{-/-}$ testes appear at P20 (Fig. 1A-B, D-E) and are obvious by P28. Indeed, when compared to the well-organized epithelium in the first wave of spermatogenesis from control testes (Fig. 1G), germ cells in *Claudin11*$^{-/-}$ testes appear abnormally localized. Round clusters of cells are observed closely apposed to the basal side of the seminiferous epithelium and the testis tubular lumen is poorly defined and is filled with round spermatids or cell clusters (Fig. 1H). Moreover, while elongated spermatids appear in some tubes of P28 control testes, only scarce ectopically localized round spermatids are present in *Claudin11*$^{-/-}$ testes (Fig. 1 G-H). In addition, elongated spermatids are never observed in *Claudin11*$^{-/-}$ testes at P28 or P60, and spermatogenesis does not proceed beyond meiosis, which is consistent with published findings (18). The phenotype is accentuated at P60, and PAS-positive material is observed inside the cell clusters indicative of the presence of glycoproteins (Fig. 1J-K).

Because *Claudin11* expression has been reported during fetal testis development (23), we compared the temporal appearance of the *Claudin11*$^{-/-}$ testes phenotype with that of protein expression in control testes (Fig. 1C, E, I). Although claudin11 is not detected by immunohistochemistry at P10 (data not shown), it is obvious in some tubes at P13, with labeling extending from the basal membrane to the lumen (Fig. 2C). Such staining is consistent with the localization of claudin11 to plasma membrane and the polarization of Sertoli cells from P20 onwards (Fig. 1F, I). Thus, the appearance of the first histological defects in *Claudin11*$^{-/-}$ testes closely parallels the kinetics of claudin11 expression in control testes. Testis weight in *Claudin11*$^{-/-}$ mice is normal up to P28 (Fig. 1L), which suggests defects at the organ weight level are delayed compared to the histological level.

Cell clusters are comprised of Sertoli cells

Histological sections reveal that nuclei from the vast majority of cells in adluminal cell clusters are clear and contain 1-3 nucleoli, which is reminiscent of normal Sertoli cell morphology (data not shown). However, in P60 *Claudin11*$^{-/-}$ testes, mixed cell nuclei are observed in the clusters (Fig. 1K). To identify the cells comprising these clusters, we

performed immunohistochemistry for several germ cell markers (Fig. 2): the Ddx4 protein (Mouse Vasa Homolog) is expressed in primary spermatocyte and more differentiated cells (54) (Fig. 2A), Clgn is expressed in early pachytene spermatocytes to step 14 spermatids (D) (63), vitronectin (30) and claudin1 (data not shown) are expressed in the acrosomes of spermatids. The absence of these markers demonstrates that cell clusters sloughing from the epithelium of *Claudin11*$^{-/-}$ testes do not contain germ cells (Fig. 2B-C, E, F and data not shown), although a few germ cells are found in some cell clusters from P60 – P180 mice (data not shown and Fig. 7I). By contrast, immunolabeling of Gata4, which identifies Sertoli cells inside the seminiferous epithelium (Fig 2G) (27, 57) clearly indicates that clusters are comprised of Sertoli cells (Fig. 2H-I).

Increased apoptosis in testis of *Claudin11*$^{-/-}$ mice

Although claudin11 expression in testis is Sertoli cell-specific, the primary defect in *Claudin11*$^{-/-}$ mice is that of a failure of spermatogenesis. Apoptosis is the dominant pathway for eliminating germ cells whenever the supporting Sertoli cells are unable to provide a supportive environment for their development (41); thus, we characterized the fate of germ cells using TUNEL labeling (Fig. 3). Quantification of TUNEL-labeled cells in *Claudin11*$^{-/-}$ testis shows a significant ($p < 0.05$) increase in the incidence of apoptosis at P20 and P28 compared to age-matched controls (Fig. 3A-E). The proportion of round tubes containing one or more TUNEL-positive cell is increased 1.5-fold ($p < 0.05$) in *Claudin11*$^{-/-}$ testes at P15 (Fig. 3E), suggesting an early impact of the absence of claudin11 on germ cell development. Apoptosis reaches a peak at P20 and is maintained through P28, but remains elevated at P60 and is not statistically different from levels at P20. In addition, abundant vesicles of fragmented TUNEL positive-DNA are detected in the cytoplasm of sloughing Sertoli cells (Fig. 3D), which likely indicates that Sertoli cells actively phagocytose degenerating germ cells. These kinetics are consistent with the notion that germ cell differentiation, not stem cell renewal, is perturbed by the absence of Sertoli cell TJs.

To further dissect the fate of germ cells in *Claudin11*$^{-/-}$ testes, sections were immunostained with phosphorylated histone H3 (Ph-H3) (Fig. 4). Ph-H3 is normally expressed in mitotic spermatogonia and in diplotene spermatocytes approaching cell division at stages XI and XII (10). Immunolabeling of Ph-H3 at P15, P28 and P60 show no obvious changes in mitotic spermatogonia or meiotic spermatocytes (small magnifications not shown; Fig. 4A-F) from the proportions of round tubes containing one or more Ph-H3 positive cells (Fig. 4G). By contrast, the number of Ph-H3 positive cells per round tube increase from P28 to P60 in control testes but remains constant in *Claudin11*$^{-/-}$ testes (Fig. 4C-F, H). Consequently, the total number of Ph-H3 positive cells decreases in *Claudin11*$^{-/-}$ testes (Fig. 4H) at P28 and P60. Together, these data suggest that amplification of the germ cell population resulting from active spermatogenesis does not occur in absence of claudin11 at the inter-Sertoli BTB.

Dynamics of Sertoli cell sloughing in *Claudin11*$^{-/-}$ testes

To determine how a lack of claudin11 might impact Sertoli cell topography within the seminiferous epithelium, sections were immunolabeled with Gata4 (Fig. 5). In control testes, Sertoli cell nuclei are positioned at the basement membrane of the seminiferous epithelium as expected. In *Claudin*$^{-/-}$ testes, the nuclei are localized toward the centre of the tube as early as P13 (Fig. 5A, B), which coincides with the beginning of claudin11 expression in control testes (Fig. 1C). At P28 (Fig. 5) - also seen at P20 (data not shown) - basally located Sertoli cells are observed as well as several abnormal Sertoli cell arrangements (Fig. 5C-F). These include groupings of Sertoli cells adjacent to the base of the tube (Fig. 5D), round clusters

with few cells attached to the basement membrane (Fig. 5E) and completely detached Sertoli cell clusters filling the tube lumen (Fig. 5F). These data are indicative of dynamic Sertoli cell sloughing from their basal sites into the lumen of the tube.

In this light, we hypothesize that Sertoli cells may migrate along the basement membrane to form small groups which then detach, or they may form clusters by cell division and thereafter detach. To distinguish between these possibilities, we examined changes in the number of Gata4 labeled Sertoli cells from P15 to P60 (Fig. 6A-C). Consistent with the temporal development of the phenotype, the number of Sertoli cells per cluster rises from P15 to P28 and is maintained at this level through P60 in *Claudin11*$^{-/-}$ testes (Fig. 6A). In addition, the proportion of round tubes containing detached Sertoli cells almost doubles between P15 and P60 ($p < 0.05$). Indeed, more than 80% of the tubes contain Sertoli cell clusters at P60 (Fig. 6B).

While the number of Sertoli cells per round tube decreases from P15 to P60 in control testes (probably as a result of dilution due to massive increase of the germ cell population within the tubules as the animals mature), the size of this population remains almost constant in *Claudin11*$^{-/-}$ testes (Fig. 6C). The number of Sertoli cells per round tube in control and *Claudin11*$^{-/-}$ testes is similar at P15 and at P28 if both peripherally- and cluster-located Sertoli cells are considered. At P60, the number of peripherally-located Sertoli cells is similar in control and *Claudin11*$^{-/-}$ testes, but higher in *Claudin11*$^{-/-}$ testes when considering total Sertoli cell numbers. Together, these data suggest a continuous renewal of Sertoli cells to compensate for their losses from detachment and shedding into the lumen.

Sertoli cells undergo cell division in *Claudin11*$^{-/-}$ testes

Sertoli cells cease dividing in immature animals during the first 2 weeks after birth, which is concomitant with the appearance of meiotic germ cells and formation of the lumen (28, 56). To determine the cell cycle status of Sertoli cells, we performed an in-depth survey of Gata4-labeled Sertoli cells (Fig. 6E-J). In control testes, Gata4 labeling of Sertoli cell nuclei is homogenous, with the exception of nucleoli (Fig. 6E, H) and similarly labeled Sertoli cells are found in P28 (Fig. 6D-F) and P60 (not shown) *Claudin11*$^{-/-}$ testes. In addition, compacted chromatin in Gata4-positive nuclei is also observed, together with the characteristic meiotic figures of germ cells (Fig. 6F).

Juxtaposed Sertoli cells in the plane parallel to the basement membrane in *Claudin11*$^{-/-}$ testes (Fig. 6E), suggest that this cell population may be dividing. To unambiguously identify dividing Sertoli cells, we used in vivo BrdU-incorporation prior to the fixation and tissue processing (Fig. 6G-H). Comparison of the Gata4-positive Sertoli cell and BrdU-positive dividing cell populations in wild type testes reveals the canonical complementary pattern of Sertoli cell and spermatogonia (Fig. 6G). This is a hallmark of stage VIII tubes, wherein spermatogonia proliferate and leptotene spermatocytes traverse the BTB into the adluminal compartment for further development (12, 27, 29, 29, 32). In *Claudin11*$^{-/-}$ testes, stage VIII tubes contain Gata4-positive Sertoli cells and BrdU-labeled spermatogonia, indicating that the lack of claudin11 expression does not hamper the spermatogenic cycle, or at least the cyclical entry of spermatogonia into mitosis at stage VIII (39). However, double labeled cells are also present at the periphery of some tubes (Fig. 6H), which demonstrates that Sertoli cells are proliferating in *Claudin11*$^{-/-}$ testes. Importantly, we do not observe BrdU labeling of cell clusters, indicating that Sertoli cell division occurs prior to cluster formation and shedding into the lumen.

Loss of Sertoli cell polarity but maintenance of differentiation markers

In Fig. 5, we observe that Sertoli cells in *Claudin11*$^{-/-}$ testes change shape in the course of cell cluster sloughing. Thus, the nuclei of basal Gata4-labelled Sertoli cells are round or triangular, while Sertoli cells located at the periphery of clusters have round nuclei and those within clusters have smaller and elongated or comma-shaped nuclei. Such shapes are reminiscent of fibroblasts (Fig. 7A), and indicate a loss of cell polarity and possibly differentiation status. To examine these possibilities, we analyzed several Sertoli cell differentiation markers. Vimentin, androgen receptor and N-cadherin labeling (Fig. 7B-E, H-I and data not shown) demonstrates that *Claudin11*$^{-/-}$ Sertoli cells retain mature markers, even in luminal cell clusters from P180 testes when the number of germ cells and, consequently, testis weight is in decline. We also observe vimentin-positive Sertoli cell clusters in the epididymides of *Claudin11*$^{-/-}$ mice (Fig. 7F-G), suggesting that they are cleared from the testes in similar fashion to sperm cells. Consistent with the absence of sperm, the lumen of most epididymides are empty (Fig. 7G). By contrast, epididymides from control animals are filled with sperm cells (Fig. 7F).

Molecular characterization of *Claudin11*$^{-/-}$ testes using microarrays

To better understand the molecular consequences of the absence of claudin11 on Sertoli cells, we performed a microarray analysis of whole testis mRNA from P20 *Claudin11*$^{-/-}$ mice. Littermate *Claudin11*$^{+/-}$ mice were used as controls, which are fertile and otherwise indistinguishable from wild type mice in all studies we have performed. The choice of P20 stems from two main considerations; testis weight and germ cell composition are similar in *Claudin11*$^{-/-}$ and control groups; Sertoli cells had begun to detach from the basement membrane. The strategy was based on a substractive approach following a dye swap experimental procedure to catch the most differentially up and down-regulated genes. Microarray analysis identified 108 genes significantly up- and 98 down-regulated by > 1.3-fold in *Claudin11*$^{+/-}$ compared with *Claudin11*$^{-/-}$ testes (SAM procedure with FDR < 5%). Importantly, *Claudin11* is the most down-regulated gene (Table 2), which accords with the genotype of *Claudin11*$^{-/-}$ mice. In addition, we selected 6 up- and 1 down-regulated genes on the basis of the amount of expression and their possible biological significance and confirmed differences in the expression levels by quantitative PCR analysis (Table 2). In agreement with the histological data (Fig. 1D-E), amongst the up-regulated genes, 22 (20.4 %) were inferred to Sertoli cells and 4 to germ cells (3.7 %); amongst the down regulated genes, 28 (29.6 %) were inferred to germ cells, most often spermatocytes (Supplemental Table 1). Also consistent with the immunohistological data, the *Vimentin* gene was already up-regulated in P20 *Claudin11*$^{-/-}$ testes. Interestingly, typical Sertoli cell markers such as Etv5 (also known as Erm), Sox8, Sox9, Desert hedgehog, transferrin or Kit ligand displayed a similar expression in control and *Claudin11*$^{-/-}$ testes (data not shown). Notably, WebGestalt analysis of microarray data revealed a statistical enrichment of TJ ($p = 1.36\ 10^{-6}$), regulation of actin cytoskeleton ($p = 2.72\ 10^{-3}$), cell cycle ($p = 1.14\ 10^{-4}$), gluthatione metabolism ($p = 2.75\ 10^{-7}$), adherens junction ($p = 1.84\ 10^{-3}$) KEGG pathways. Interestingly, expression of genes of the tight and adherens junctions and actin and intermediate filament cytoskeleton pathways were coordinately up-regulated (16 of 18 genes and 14 of 15 genes, respectively).

DISCUSSION

The present data highlight the critical role of claudin11 in the maintenance of Sertoli cell epithelial differentiation. Indeed, in the absence of claudin11, Sertoli cells differentiate but tend to re-enter the cell cycle rather than permanently arresting as non-mitotic quiescent cells. They form homogeneous clusters, lose their contact with basement membrane, detach

from the seminiferous epithelium and acquire a fibroblast-like cell shape. At the molecular level, the absence of claudin11 expression induces selective changes in several cell-junction related genes, specifically TJ genes, as well as genes associated with the cytoskeleton.

A growing number of genes associated with male infertility have been generated using homologous recombination in embryonic stem cells (11, 52). A frequent feature of mouse models of infertility is germ cell defect consecutive to either depletion of stem cells, meiosis arrest, or spermiogenesis default. Disruption of meiosis notably induces massive germ cell apoptosis and elimination by their phagocytosis by Sertoli cells, resulting in histological characteristics such as vacuoles in Sertoli cell cytoplasm and multinucleated spermatids. As well, the primary impact of somatic cell physiology disruption (very often through impairment of hormonal action) is germ cell development damage. By comparison, gene ablation of genes encoding TJ proteins such as Occludin, ZO-1 and JAM1 display variable phenotypes ranging from Sertoli cell only syndrome of the old adult to the apparent absence of a testicular phenotype (32, 45, 53). Together, our results demonstrate that claudin11 plays a key role in both Sertoli cell physiology and spermatogenesis.

Amongst mouse models of infertility, very few involve a primary defect in the Sertoli cell maturation process, i.e., proliferation and differentiation, and none of them results in the uncoupling between these two states. For example, delayed Sertoli cell cluster formation has been reported in adult *Dazl*$^{-/-}$ mice, where the primary defect is a failure of stem spermatogonia to differentiate into spermatogonia committed to spermatogenesis (43), and in rats treated with busulphan, which interferes with germ cell renewal (29, 48). In mice with a Sertoli cell-specific gene ablation of *Connexin43*, continued Sertoli cell proliferation in adulthood and clusters of sloughed cells comprised of Sertoli cells have been observed. However, Sertoli cell sloughing is concurrent with a dramatic early depletion of germ cells and Sertoli cell differentiation is inhibited (17, 45). By contrast, Sertoli cell sloughing in *Claudin11*$^{-/-}$ testes is conspicuous from P13, when there is little evidence of germ cell pathology or apoptosis. At P20, tubes are filled with germ cells and germ cell depletion is not obvious until germ cells fail to progress beyond meiosis. Consequently, we speculate that Sertoli cell detachment is a primary defect of *Claudin11*$^{-/-}$ testes, and that the lack of *Claudin11* does not preclude maturation of Sertoli cells as shown in the microarray study.

Several lines of evidence indicate that claudin11 expression and TJ permeability are directly regulated by androgen signaling. Adult mice that are deficient for androgen receptor only in Sertoli cells (S-AR$^{-/y}$) display Sertoli cell disorganization similar to that observed in *Claudin11*$^{-/-}$ mice. This is associated with a sharp decrease in *Claudin11*, *Occludin* and *Gelsolin* mRNA levels as well as an increase in *Vimentin* expression (61). Mice expressing a mutant form of the androgen receptor display abnormal expression of TJ proteins and Sertoli cell cytoskeleton genes (66). Detachment of Sertoli cells has been reported in anti-androgen cimetidin-treated rats (46). Collectively, these *in vivo* mouse models support the physiological relevance of *in vitro* demonstrations that *Claudin11* expression is regulated by androgens (26).

In contrast to cimetidine-treated rats, in which Sertoli cell detachment from the basement membrane parallels Sertoli cell apoptosis (46), claudin11 deficiency is associated with Sertoli cell proliferation and germ cell apoptosis and phagocytosis. Microarray data from these animals reveal an induction of detoxification machinery in Sertoli cells [up-regulation of *Gstm1* and *Gstm6*, (5, 37)] and a suppression of detoxification machinery in germ cells [down-regulation of *Gstm3* (18)]. It is tempting to speculate that these changes constitute an

initial trigger for germ cell apoptosis. Tight junctions are critical regulators of the microenvironment in epithelia and determine paracellular barrier properties. Because claudin11 forms TJs by itself (24, 40, 51), its loss disrupts Sertoli cell TJs and perturbs the seminiferous epithelium micro-environment. This is analogous to previous studies showing that germ cell apoptosis is an indirect effect of a leaky BTB caused by the absence of a protease inhibitor (30).

Alternatively, germ cell apoptosis from the loss of TJs may occur concurrently with an intrinsic Sertoli cell defect. This is similar to a loss of fetal androgen, which disrupts Sertoli cell maturation and impedes the ability of these cells to protect germ cells (4). Phagocytosing Sertoli cells generate large amounts of free-radicals (2), which is compensated by induction of antioxidation pathways. However, germ cells are poorly equipped to combat free radical attack and are particularly vulnerable because their plasma membrane is rich in polyunsaturated fatty acids (2, 3). Oxidative stress has been linked to apoptosis (16); thus, it could be hypothesized that the germ cell apoptosis system may run off like a snowball effect. However, the two hypotheses do not exclude each other.

In light of the possibility that the Sertoli cell phenotype stems directly from claudin11 deficiency, we hypothesize that the underlying mechanism involves Sertoli cell re-entry into the cell cycle. During development, mouse Sertoli cells normally stop dividing commensurate with assembly of the BTB and the beginning of spermatogenesis. This leads to an almost quiescent state during the second week of life in mice (8, 28, 56). *In vitro*, recent studies show that P7-P8 and adult mouse Sertoli cells can resume mitosis, and that this phenomenon is accentuated by the absence of connexin43, suggesting that Sertoli cells may be arrested proliferative cells rather than terminally differentiated somatic cells (1, 19). In the current study, we show that Sertoli cells lacking claudin11 *in vivo* incorporate BrdU at P28 and P60, thereby demonstrating that they have re-entered the cell cycle, albeit at a low proliferation rate. Nevertheless, Sertoli cell number in *Claudin11*$^{-/-}$ mice is comparable to controls at P28 and slightly increased at P60. Additionally, Sertoli cells are still present in 6 month old *Claudin11*$^{-/-}$ testes despite their continuous sloughing from the epithelium.

Interestingly, functional TJs assemble when Sertoli cells cease to divide, which suggests that BTB formation could regulate Sertoli cell cycle. Consistent with this notion, the up-regulation of cell cycle genes observed in the microarray data are partially attributable to Sertoli cell proliferation rather than only to germ cells committed to apoptosis. Indeed, amongst cell cycle up-regulated genes, *Rab12* is expressed by Sertoli cells while *Cdk5* is germ cell-specific (25, 49). Down-regulated cell cycle genes in *Claudin11*$^{-/-}$ testes including *Ccnb2* and *Ccna1* have mostly been described in meiotic germ cells (9, 31). Thus, we hypothesize that the assembly of claudin 11 TJs helps to ensure that Sertoli cells are contact inhibited and remain quiescent.

In the current study, we find that the Sertoli cell phenotype in the seminiferous tubules of *Claudin11*$^{-/-}$ mice includes the acquisition of a fibroblastic cell shape in cell clusters. Changes in cell shape are often associated with altered cytoskeletal gene expression and it is satisfying that our microarray analysis reveals a number of changes in the expression of Sertoli cell-specific genes including *Vinculin*, *αActinin4*, *Spectrin α2* and *Vimentin*. Conceivably, the induction of these genes may be related to a germ cell apoptosis-related shift in the composition of the epithelium; however, several canonical Sertoli cell markers are unchanged, which argues against a significant change in the Sertoli cell:germ cell ratio. While de-differentiation of Sertoli cells might be an expected outcome of persistent proliferation and

reorganization of the vimentin network, our microarray data show that these cells maintain the expression of several mature Sertoli cell markers, including the androgen-receptor, and express high levels of *Gata1* and *Fshr*, (50) at P20. Therefore, we find no evidence that Sertoli cells are committed to a dedifferentiation process in the absence of TJs.

Alternatively, Sertoli cells could become committed to a pre-neoplasic process in the absence of TJs. In addition to Sertoli cell proliferation, *Claudin11*$^{-/-}$ testes express high levels of *Metadherin*, which is a known tumor cell marker (6). However, dividing Sertoli cells are only observed at the periphery of tubules, and not in luminal cell clusters, indicating that these cells become quiescent before they slough. Moreover, instead of invading the entire testis, Sertoli cell clusters are cleared via the normal conducts and are found in the epididymis. At 6 months, testis histology is not significantly different from that at 2 months, but is dramatically different from typical Sertoli cell tumors (64, 65). Finally, testicular tumors have not been observed in our mouse colony in more than 10 years and despite maintaining mice beyond 12 months of age (A.G., unpublished). Although several studies have demonstrated the induction or suppression of various *CLAUDIN* genes in different cancers, in support of a relationship between TJ-based barrier function and cell proliferation (24, 40, 51), our data strongly suggest that the absence of claudin11 in Sertoli cells does not commit these cells to a neoplastic transformation.

A surprising finding in *Claudin11*$^{-/-}$ mice involves the ability of mature Sertoli cells to re-aggregate after sloughing. Aggregation of these cells is the first sign of fetal testis differentiation (33) but this behavior is probably independent of *Claudin11* expression because testis development and morphology at P10 are normal in *Claudin11*$^{-/-}$ mice. Although mechanisms regulating homophilic recognition and cell aggregation in Sertoli cells are unclear, changes in expression of intercellular junction and cytoskeletal genes from our microarrays suggest a role for claudin11 in intracellular signaling, including a feedback loop for the cell to compensate for excessive TJ permeability. Regulation of adherens junction proteins such as N-cadherin (data not shown) may be sufficient for Sertoli cell aggregation, with claudin11 mediating polarization. Alternatively, high levels of clusterin expression may contribute to Sertoli cell aggregation. *Clusterin* is the most highly stimulated gene in our microarrays study and its encoded protein is known to cause aggregation of Sertoli cells from immature rats and TM-4 cells from mouse testis (17). In addition, induction of the actin and intermediate filament genes may be related to the Sertoli cell shape changes and their sloughing into the lumen.

Among mouse models of male infertility, *Claudin11*$^{-/-}$ mice display a unique testis phenotype in which the primary defect is epithelial disorganization, mitosis, and detachment of Sertoli cells from the basement membrane in the face of adult differentiation marker expression. These data notwithstanding, in the testis, the absence of TJs and subsequent epithelial-to-mesenchymal transition of Sertoli cells does not reflect a transformation toward neoplasia and tumor formation. Furthermore, although more than one claudin family member has been shown at the BTB (35), our demonstrate a lack of functional redundancy at the BTB.

ACKNOWLEDEMENTS

We thank Drs. T. Noce and H. Tanaka for providing for Ddx4 and Cgln antibodies, respectively. We thank Mr Kevin Olson, Center for Molecular Medicine and Genetics, WSU, for technical assistance in the collection of tissues from the *Claudin11* mouse colony. This work was supported by Inserm, Inra, University Lyon I, and partly from grants to BLMB by ANR (ANR-06-PNRA-006) and AFSSET (EST-2006/1/33), and to A.G. by NIDCD, NIH (DC006262).

FIGURE LEGENDS

Fig. 1. Chronology of the testis phenotype in *Claudin11*$^{-/-}$ mice. Testicular sections of P13 (A-C), P20 (D-F), P28 (G-I) and P60 (J, K) from control (A, D, G, J, C, F, I) and *Claudin11*$^{-/-}$ (B, E, H, K) mice were processed for PAS histological staining (A-B, D-E, G-H, J-K) and claudin11 immunohistochemistry (C, F, I). Control (black) and *Claudin11*$^{-/-}$ (white) **t**estis weight (n = 3) (L). Asterisks indicate statistical significance ($p < 0.001$) by One-way ANOVA followed by Tukey's post hoc testing. Bars : 100 µm.

Fig. 2. Nature of cell clusters. Immunolabeling of germ cell markers Ddx4 (A-C), calmegin (Clgn) recognized by the TRA369 antibody (D-F) and Sertoli cell marker Gata4 (G-I) of P28 control (A, D, G) and *Claudin11*$^{-/-}$ (B-C, E-F, H-I) testes show that cell cluster found in the lumen of *Claudin11*$^{-/-}$ testes are Sertoli cells. Bars : 100 µm.

Fig. 3 High incidence of germ cell apoptosis in *Claudin11*$^{-/-}$ testes. TUNEL analysis of control (A) and *Claudin11*$^{-/-}$ (B, D) testes at P20 (A-B) show increased germ cell apoptosis in *Claudin11*$^{-/-}$ testes. In (C), Counts of round seminiferous tubes containing at least one TUNEL-positive cell. Data show that first significant increase was seen at P15. Values are mean +/- S.E.M. of 3-6 animals. Asterisks indicate statistical significance ($p < 0.001$) by One-way ANOVA followed by Holm-Sidak's post hoc testing. In addition to TUNEL-positive germ cells localized in the seminiferous epithelium, small vesicles of fragmented TUNEL positive-DNA reminiscent of phagocytosis are abundant in cytoplasm of sloughing Sertoli cells (arrows in D). Asterisks indicate statistical significance ($p < 0.001$) by One-way ANOVA followed by Holm-Sidak's post hoc testing. Bars : 100 µm.

Fig. 4. Exhaustion of germ cells. Immunolabeling of Phospho-H3 in primary spermatocytes of P15 (A, B), P28 (C, D) and P60 (E-F) control (A, C, E) and *Claudin11*$^{-/-}$ testes (B, D, F) show germ cells in the division phases. Analysis of the percentage of round tubes that contain at least one Phospho-H3-positive cell (G) together with the number of Phospho-H3 positive cell per round tube (H) shows the progressive loss of germ cells. Asterisks indicate statistical significance ($p < 0.001$) by Mann-Whitney rank test (G) or Kruskal-Wallis One-way ANOVA followed by Dunn's pairwise multiple comparison testing (H). Bars : 100 µm.

Fig. 5. Dynamics of Sertoli cell sloughing. Immunolabeling of Gata4 of P13 (A-B) and P28 (C-F) control (A, C) and *Claudin11*$^{-/-}$ (B, D-F) testes shows the progressive sloughing of Sertoli cells from P13 onward and from the basal pole (D) to the lumen (E-F) of the seminiferous tube. Bars : 100 µm.

Fig. 6. Sertoli cell number evolution. Counts of Gata4-positive cells in round tubes show that both the number of Sertoli cells per cluster (A) and the percentage of seminiferous tubes that contain clusters (B) increase with age in *Claudin11*$^{-/-}$ testes. The comparison of the number of Sertoli cells located at the periphery of control round tubes with the number of Sertoli cells located at the periphery of round tubes and with the total number of Sertoli cell

per round tube in *Claudin11*$^{-/-}$ testes show the relative maintenance of Sertoli cells at P28 and the relatively high total number of Sertoli cells at P60 (C). Asterisks indicate statistical significance ($P<0.001$) by One-way ANOVA followed by Tukey's post hoc testing. Close examination of Gata4 labeling of control (D) and *Claudin11*$^{-/-}$ (E-F) testis sections at P28 (D-F) show the chromatin aspect of Gata4-labeled Sertoli cell nuclei, from dense compact (arrowheads) to compacted (arrows), compared with the compacted chromatin of meiotic spermatocytes (large arrows). Double labeling of Gata4-positive Sertoli cells (green, arrowheads) and BrdU-positive dividing cells (red) in control (G) and *Claudin11*$^{-/-}$ (H) P28 testes show the presence of double labeled dividing Sertoli cells (large arrows), compared to dividing germ cells (arrows). Asterisks depict Gata4-positive Sertoli cell clusters. Bars: 50 µm in D-F and 100 µm in G-H.

Fig. 7. Sertoli cell loss of polarity. Immunolabeling of Gata4 in Sertoli cell nuclei of P28 (A) *Claudin11*$^{-/-}$ testes shows the progressive change in Sertoli nuclei shape, from round (arrowhead) to fibroblastic-like elongated (arrows). Immunolabeling of vimentin in Sertoli cells of P28 (B, C), P60 (D-G) and 6 months (H, I) control (B, D, F, H) and *Claudin11*$^{-/-}$ (C, E, G, I) testes (B-E, H-I) and epididymes (F-G) shows the maintenance of vimentin expression in detaching Sertoli cell clusters from the seminiferous tube to the epididimys lumen in *Claudin11*$^{-/-}$ animals. Bars : 20µm in A and 100µm in B-I.

REFERENCES

1. **Ahmed, E. A., A. D. Barten-van Rijbroek, H. B. Kal, H. Sadri-Ardekani, S. C. Mizrak, A. M. van Pelt, and D. G. de Rooij.** 2009. Proliferative Activity In Vitro and DNA Repair Indicate that Adult Mouse and Human Sertoli Cells Are Not Terminally Differentiated, Quiescent Cells. Biol Reprod.
2. **Bauche, F., M. H. Fouchard, and B. Jegou.** 1994. Antioxidant system in rat testicular cells. FEBS Lett **349:**392-6.
3. **Beckman, J. K., and J. G. Coniglio.** 1979. A comparative study of the lipid composition of isolated rat Sertoli and germinal cells. Lipids **14:**262-7.
4. **Benbrahim-Tallaa, L., B. Siddeek, A. Bozec, V. Tronchon, A. Florin, C. Friry, E. Tabone, C. Mauduit, and M. Benahmed.** 2008. Alterations of Sertoli cell activity in the long-term testicular germ cell death process induced by fetal androgen disruption. J Endocrinol **196:**21-31.
5. **Beverdam, A., T. Svingen, S. Bagheri-Fam, P. Bernard, P. McClive, M. Robson, M. B. Khojasteh, M. Salehi, A. H. Sinclair, V. R. Harley, and P. Koopman.** 2009. Sox9-dependent expression of Gstm6 in Sertoli cells during testis development in mice. Reproduction **137:**481-6.
6. **Britt, D. E., D. F. Yang, D. Q. Yang, D. Flanagan, H. Callanan, Y. P. Lim, S. H. Lin, and D. C. Hixson.** 2004. Identification of a novel protein, LYRIC, localized to tight junctions of polarized epithelial cells. Exp Cell Res **300:**134-48.
7. **Brokelmann, J.** 1963. Fine structure of germ cells and Sertoli cells during the cycle of the seminiferous epithelium in the rat. Z Zellforsch Mikrosk Anat **59:**820-50.
8. **Byers, S., R. Graham, H. N. Dai, and B. Hoxter.** 1991. Development of Sertoli cell junctional specializations and the distribution of the tight-junction-associated protein ZO-1 in the mouse testis. Am J Anat **191:**35-47.
9. **Chapman, D. L., and D. J. Wolgemuth.** 1993. Isolation of the murine cyclin B2 cDNA and characterization of the lineage and temporal specificity of expression of the B1 and B2 cyclins during oogenesis, spermatogenesis and early embryogenesis. Development **118:**229-40.
10. **Cobb, J., M. Miyaike, A. Kikuchi, and M. A. Handel.** 1999. Meiotic events at the centromeric heterochromatin: histone H3 phosphorylation, topoisomerase II alpha localization and chromosome condensation. Chromosoma **108:**412-25.
11. **Cooke, H. J., and P. T. Saunders.** 2002. Mouse models of male infertility. Nat Rev Genet **3:**790-801.
12. **Cooke, V. G., M. U. Naik, and U. P. Naik.** 2006. Fibroblast growth factor-2 failed to induce angiogenesis in junctional adhesion molecule-A-deficient mice. Arterioscler Thromb Vasc Biol **26:**2005-11.
13. **Devaux, J., and A. Gow.** 2008. Tight junctions potentiate the insulative properties of small CNS myelinated axons. J Cell Biol **183:**909-21.
14. **Dym, M., and D. W. Fawcett.** 1970. The blood-testis barrier in the rat and the physiological compartmentation of the seminiferous epithelium. Biol Reprod **3:**308-26.
15. **Flickinger, C., and D. W. Fawcett.** 1967. The junctional specializations of Sertoli cells in the seminiferous epithelium. Anat Rec **158:**207-21.
16. **Franco, R., R. Sanchez-Olea, E. M. Reyes-Reyes, and M. I. Panayiotidis.** 2008. Environmental toxicity, oxidative stress and apoptosis: Menage a Trois. Mutat Res.
17. **Fritz, I. B., K. Burdzy, B. Setchell, and O. Blaschuk.** 1983. Ram rete testis fluid contains a protein (clusterin) which influences cell-cell interactions in vitro. Biol Reprod **28:**1173-88.

18. **Fulcher, K. D., J. E. Welch, D. G. Klapper, D. A. O'Brien, and E. M. Eddy.** 1995. Identification of a unique mu-class glutathione S-transferase in mouse spermatogenic cells. Mol Reprod Dev **42:**415-24.
19. **Gilleron, J., D. Carette, P. Durand, G. Pointis, and D. Segretain.** 2009. Connexin 43 a potential regulator of cell proliferation and apoptosis within the seminiferous epithelium. Int J Biochem Cell Biol **41:**1381-90.
20. **Gow, A., C. Davies, C. M. Southwood, G. Frolenkov, M. Chrustowski, L. Ng, D. Yamauchi, D. C. Marcus, and B. Kachar.** 2004. Deafness in Claudin 11-null mice reveals the critical contribution of basal cell tight junctions to stria vascularis function. J Neurosci **24:**7051-62.
21. **Gow, A., C. M. Southwood, J. S. Li, M. Pariali, G. P. Riordan, S. E. Brodie, J. Danias, J. M. Bronstein, B. Kachar, and R. A. Lazzarini.** 1999. CNS myelin and sertoli cell tight junction strands are absent in Osp/claudin-11 null mice. Cell **99:**649-59.
22. **Gumbiner, B. M.** 1993. Breaking through the tight junction barrier. J Cell Biol **123:**1631-3.
23. **Hellani, A., J. Ji, C. Mauduit, C. Deschildre, E. Tabone, and M. Benahmed.** 2000. Developmental and hormonal regulation of the expression of oligodendrocyte-specific protein/claudin 11 in mouse testis. Endocrinology **141:**3012-9.
24. **Hewitt, K. J., R. Agarwal, and P. J. Morin.** 2006. The claudin gene family: expression in normal and neoplastic tissues. BMC Cancer **6:**186.
25. **Iida, H., M. Noda, T. Kaneko, M. Doiguchi, and T. Mori.** 2005. Identification of rab12 as a vesicle-associated small GTPase highly expressed in Sertoli cells of rat testis. Mol Reprod Dev **71:**178-85.
26. **Kaitu'u-Lino, T. J., P. Sluka, C. F. Foo, and P. G. Stanton.** 2007. Claudin-11 expression and localisation is regulated by androgens in rat Sertoli cells in vitro. Reproduction **133:**1169-79.
27. **Ketola, I., N. Rahman, J. Toppari, M. Bielinska, S. B. Porter-Tinge, J. S. Tapanainen, I. T. Huhtaniemi, D. B. Wilson, and M. Heikinheimo.** 1999. Expression and regulation of transcription factors GATA-4 and GATA-6 in developing mouse testis. Endocrinology **140:**1470-80.
28. **Kluin, P. M., M. F. Kramer, and D. G. de Rooij.** 1984. Proliferation of spermatogonia and Sertoli cells in maturing mice. Anat Embryol (Berl) **169:**73-8.
29. **Kopecky, M., V. Semecky, and P. Nachtigal.** 2005. Vimentin expression during altered spermatogenesis in rats. Acta Histochem **107:**279-89.
30. **Le Magueresse-Battistoni, B.** 2007. Serine proteases and serine protease inhibitors in testicular physiology: the plasminogen activation system. Reproduction **134:**721-9.
31. **Liu, D., M. M. Matzuk, W. K. Sung, Q. Guo, P. Wang, and D. J. Wolgemuth.** 1998. Cyclin A1 is required for meiosis in the male mouse. Nat Genet **20:**377-80.
32. **Lui, W. Y., and C. Y. Cheng.** 2007. Regulation of cell junction dynamics by cytokines in the testis: a molecular and biochemical perspective. Cytokine Growth Factor Rev **18:**299-311.
33. **Magre, S., and A. Jost.** 1980. The initial phases of testicular organogenesis in the rat. An electron microscopy study. Arch Anat Microsc Morphol Exp **69:**297-318.
34. **Masri, B. A., L. D. Russell, and A. W. Vogl.** 1987. Distribution of actin in spermatids and adjacent Sertoli cell regions of the rat. Anat Rec **218:**20-6.
35. **Meng, J., R. W. Holdcraft, J. E. Shima, M. D. Griswold, and R. E. Braun.** 2005. Androgens regulate the permeability of the blood-testis barrier. Proc Natl Acad Sci U S A **102:**16696-700.

36. **Mirza, M., C. Petersen, K. Nordqvist, and K. Sollerbrant.** 2007. Coxsackievirus and adenovirus receptor is up-regulated in migratory germ cells during passage of the blood-testis barrier. Endocrinology **148:**5459-69.
37. **Mukherjee, S. B., S. Aravinda, B. Gopalakrishnan, S. Nagpal, D. M. Salunke, and C. Shaha.** 1999. Secretion of glutathione S-transferase isoforms in the seminiferous tubular fluid, tissue distribution and sex steroid binding by rat GSTM1. Biochem J **340 (Pt 1):**309-20.
38. **Nicander, L.** 1967. An electron microscopical study of cell contacts in the seminiferous tubules of some mammals. Z Zellforsch Mikrosk Anat **83:**375-97.
39. **Oakberg, E. F.** 1956. Duration of spermatogenesis in the mouse and timing of stages of the cycle of the seminiferous epithelium. Am J Anat **99:**507-16.
40. **Oliveira, S. S., and J. A. Morgado-Diaz.** 2007. Claudins: multifunctional players in epithelial tight junctions and their role in cancer. Cell Mol Life Sci **64:**17-28.
41. **Print, C. G., and K. L. Loveland.** 2000. Germ cell suicide: new insights into apoptosis during spermatogenesis. Bioessays **22:**423-30.
42. **Romrell, L. J., and M. H. Ross.** 1979. Characterization of Sertoli cell-germ cell junctional specializations in dissociated testicular cells. Anat Rec **193:**23-41.
43. **Russell, L.** 1977. Observations on rat Sertoli ectoplasmic ('junctional') specializations in their association with germ cells of the rat testis. Tissue Cell **9:**475-98.
44. **Russell, L. D., J. C. Goh, R. M. Rashed, and A. W. Vogl.** 1988. The consequences of actin disruption at Sertoli ectoplasmic specialization sites facing spermatids after in vivo exposure of rat testis to cytochalasin D. Biol Reprod **39:**105-18.
45. **Saitou, M., M. Furuse, H. Sasaki, J. D. Schulzke, M. Fromm, H. Takano, T. Noda, and S. Tsukita.** 2000. Complex phenotype of mice lacking occludin, a component of tight junction strands. Mol Biol Cell **11:**4131-42.
46. **Sasso-Cerri, E., and P. S. Cerri.** 2008. Morphological evidences indicate that the interference of cimetidine on the peritubular components is responsible for detachment and apoptosis of Sertoli cells. Reprod Biol Endocrinol **6:**18.
47. **Schneeberger, E. E., and R. D. Lynch.** 2004. The tight junction: a multifunctional complex. Am J Physiol Cell Physiol **286:**C1213-28.
48. **Schrans-Stassen, B. H., P. T. Saunders, H. J. Cooke, and D. G. de Rooij.** 2001. Nature of the spermatogenic arrest in Dazl -/- mice. Biol Reprod **65:**771-6.
49. **Session, D. R., M. P. Fautsch, R. Avula, W. R. Jones, A. Nehra, and E. D. Wieben.** 2001. Cyclin-dependent kinase 5 is expressed in both Sertoli cells and metaphase spermatocytes. Fertil Steril **75:**669-73.
50. **Sharpe, R. M., C. McKinnell, C. Kivlin, and J. S. Fisher.** 2003. Proliferation and functional maturation of Sertoli cells, and their relevance to disorders of testis function in adulthood. Reproduction **125:**769-84.
51. **Swisshelm, K., R. Macek, and M. Kubbies.** 2005. Role of claudins in tumorigenesis. Adv Drug Deliv Rev **57:**919-28.
52. **Toshimori, K., C. Ito, M. Maekawa, Y. Toyama, F. Suzuki-Toyota, and D. K. Saxena.** 2004. Impairment of spermatogenesis leading to infertility. Anat Sci Int **79:**101-11.
53. **Toyama, Y., M. Maekawa, and S. Yuasa.** 2003. Ectoplasmic specializations in the Sertoli cell: new vistas based on genetic defects and testicular toxicology. Anat Sci Int **78:**1-16.
54. **Toyooka, Y., N. Tsunekawa, Y. Takahashi, Y. Matsui, M. Satoh, and T. Noce.** 2000. Expression and intracellular localization of mouse Vasa-homologue protein during germ cell development. Mech Dev **93:**139-49.

55. **Tusher, V. G., R. Tibshirani, and G. Chu.** 2001. Significance analysis of microarrays applied to the ionizing radiation response. Proc Natl Acad Sci U S A **98:**5116-21.
56. **Vergouwen, R. P., S. G. Jacobs, R. Huiskamp, J. A. Davids, and D. G. de Rooij.** 1991. Proliferative activity of gonocytes, Sertoli cells and interstitial cells during testicular development in mice. J Reprod Fertil **93:**233-43.
57. **Viger, R. S., C. Mertineit, J. M. Trasler, and M. Nemer.** 1998. Transcription factor GATA-4 is expressed in a sexually dimorphic pattern during mouse gonadal development and is a potent activator of the Mullerian inhibiting substance promoter. Development **125:**2665-75.
58. **Vogl, A. W., B. D. Grove, and G. J. Lew.** 1986. Distribution of actin in Sertoli cell ectoplasmic specializations and associated spermatids in the ground squirrel testis. Anat Rec **215:**331-41.
59. **Vogl, A. W., D. C. Pfeiffer, D. Mulholland, G. Kimel, and J. Guttman.** 2000. Unique and multifunctional adhesion junctions in the testis: ectoplasmic specializations. Arch Histol Cytol **63:**1-15.
60. **Vogl, A. W., and L. J. Soucy.** 1985. Arrangement and possible function of actin filament bundles in ectoplasmic specializations of ground squirrel Sertoli cells. J Cell Biol **100:**814-25.
61. **Wang, R. S., S. Yeh, L. M. Chen, H. Y. Lin, C. Zhang, J. Ni, C. C. Wu, P. A. di Sant'Agnese, K. L. deMesy-Bentley, C. R. Tzeng, and C. Chang.** 2006. Androgen receptor in sertoli cell is essential for germ cell nursery and junctional complex formation in mouse testes. Endocrinology **147:**5624-33.
62. **Weber, J. E., T. T. Turner, K. S. Tung, and L. D. Russell.** 1988. Effects of cytochalasin D on the integrity of the Sertoli cell (blood-testis) barrier. Am J Anat **182:**130-47.
63. **Yoshinaga, K., I. Tanii, and K. Toshimori.** 1999. Molecular chaperone calmegin localization to the endoplasmic reticulum of meiotic and post-meiotic germ cells in the mouse testis. Arch Histol Cytol **62:**283-93.
64. **Young, R. H.** 2005. Sex cord-stromal tumors of the ovary and testis: their similarities and differences with consideration of selected problems. Mod Pathol **18 Suppl 2:**S81-98.
65. **Young, R. H.** 2008. Testicular tumors--some new and a few perennial problems. Arch Pathol Lab Med **132:**548-64.
66. **Yu, Z., N. Dadgar, M. Albertelli, A. Scheller, R. L. Albin, D. M. Robins, and A. P. Lieberman.** 2006. Abnormalities of germ cell maturation and sertoli cell cytoskeleton in androgen receptor 113 CAG knock-in mice reveal toxic effects of the mutant protein. Am J Pathol **168:**195-204.
67. **Zhang, B., S. Kirov, and J. Snoddy.** 2005. WebGestalt: an integrated system for exploring gene sets in various biological contexts. Nucleic Acids Res **33:**W741-8.

Table 1. List of primer sequences used for RT-qPCR. (supplemental material)

Gene symbol	Accession no.	5'→ 3' Forward primer	5'→ 3' Reverse primer	Amplicon size
Mtdh	NM_026002	CACACAGGACACAGAAGACC	CAGAGATAGCAGGAGGAAGAG	179
Fyn	NM_008054	CAGCAAGACAAGGTGCGAAG	TGTGGGCAGGGCATCCTATAGC	205
Espn	NM_019585	AAGAGGAGCAGCGGAGGAAG	TCCTCTTTTCGCTTCTGCTC	121
Exoc4	NM_009148	AGACATCAGTGCCATGGAAG	CGTGACATGGTGATGTTGG	207
Csda	NM_011733	CACCAAAGTCCTTGGCACTG	CCTTCAACTACATCAAACTC	180
Tjp1	NM_009386	ACGCATCACAGCCTGGTTG	TGGCTCCTTCCTGTACACC	122
Lasp1	NM_010688	AGCAGCCCCTGTCTCCATAC	TCATCGATCTGCTGCACATTG	144
Rpl19	NM_009078	CTGAAGGTCAAAGGGAATGTG	GGACAGAGTCTTGATGATCTC	195

Table 2. List of selected up- and down-regulated genes in P20 Cldn11$^{-/-}$ testes.

Gene product	Gene symbol	Accession no.	Microarray fold change	Qt PCR fold change
Tight and adherens junctions				
metadherin	Mtdh	NM_026002	+ 1.60	+ 1.09 *
solute carrier family 35, member F2	Slc35f2	NM_028060	+ 1.58	
Proto-oncogene tyrosine-protein kinase FYN	Fyn	NM_008054	+ 1.55	+ 1.27 *
Espin	Espn	NM_019585	+ 1.51	+ 1.42 *
Src-substrate cortactin	Cttn	NM_007803	+ 1.51	
cingulin-like 1	Cgnl1	NM_026599	+ 1.42	
Ras homolog gene family member U	Rhou	NM_133955	+ 1.38	
Exocyst complex component 4 (Sec8l1)	Exoc4	NM_009148	+ 1.34	+ 1.22
Ras related proteinRab-12	Rab12	NM_024448	+ 1.34	
Junctional adhesion molecule 1 (JAM-A)	F11r	NM_172647	+ 1.33	
Vinculin	Vcl	NM_009502	+ 1.31	
Spectrin alpha 2 (fodrin)	Spnb2	NM_175836	+ 1.29	
Protein kinase C, delta type	Prkcd	NM_011103	+ 1.24	
Rho GTPase-activating protein	Grit	NM_177379	+ 1.22	
Alpha actinin 4	Actn4	NM_021895	+ 1.17	
Cold shock domain protein A	Csda	NM_011733	- 1.56	- 1.52 *
Claudin11	Cldn11	NM_008770	- 2.13	
Tight junction protein 1 (ZO-1)	Tjp1	NM_009386		+ 1.92 *
Actin or intermediate filament Cytoskeleton				
Gelsolin	Gsn	NM_146120	+ 1.57	
Actin-related protein 2/3 complex, subunit 1B	Arpc1b	NM_023142	+ 1.55 / +1.36	
Vimentin	Vim	NM_011701	+ 1.44	
Thymosin beta 4X chromosome	Tmsb4x	NM_021278	+ 1.38	
Actin-related protein 2/3 complex, subunit 5	Arpc5	NM_026369	+ 1.37	
plastin 3 (T-isoform)	Pls3	NM_145629	+ 1.35	
tyrosine 3-monooxygenase / tryptophan 5-monooxygenase activation protein, eta polypeptide (14-3-3 eta)	Ywhah	NM_011738	+ 1.32	
cytoplasmic FMR1 interacting protein 1 (Sra-1)	Cyfip1	NM_011370	+ 1.30	
dystroglycan 1	Dag1	NM_010017	+ 1.30	
LIM and SH3 protein 1	Lasp1	NM_010688	+ 1.29	+ 1.59 *
14-3-3 protein alpha/beta	Ywhab	NM_018753	+ 1.28	
pleckstrin homology domain containing, family H (with MyTH4 domain) member 2	Plekhh2	NM_177606	+ 1.28	
Actin-like protein 6A	Actl6a	NM_	+ 1.24	
Myosin light chain regulatory B	Mylc2b	NM_023402	+ 1.22	
Actin-like-7-beta	Actl7b	NM_025271	- 1.36	

812 **Supplemental Table 1.** List of selected up- and down-regulated genes in P20 Cldn11$^{-/-}$ testes. Asterisks depict the cell
813 specificity.
814

Gene product	Gene symbol	Accession no.	Microarray fold change
Sertoli cell products			
Clusterin precursor	Clu	NM_013492	+ 1.80
Cystatin SC	8030411F24Rik	XM_130383	+ 1.76
tescalcin	Tesc	NM_021344	+ 1.69
metadherin	Mtdh	NM_026002	+ 1.60
Gelsolin	Gsn	NM_146120	+ 1.57
calgizzarin	S100a11	NM_016740	+ 1.56
Proto-oncogene tyrosine-protein kinase FYN	Fyn	NM_008054	+ 1.55
maestro	Mro	NM_027741	+ 1.54
Espin	Espn	NM_019585	+ 1.51
Src-substrate cortactin	Cttn	NM_007803	+ 1.51
Cystatin12 (cystatin TE-1)	Cst12	XM_130487	+ 1.47
Lectin, galactose binding, soluble 1 (Galectin 1)	Lgals	NM_008495	+ 1.44
Vimentin	Vim	NM_011701	+ 1.44
Secreted protein acidic and rich in cysteine) (Osteonectin)	Sparc	NM_009242	+ 1.44
Glutathione S-transferase Mu 6	Gstm6	NM_008184	+ 1.44
Beta-defensin 19 precursor (Testis-specific beta-defensin-like protein)	Defb19	NM_145157	+ 1.43
Transmembrane protein184a	Tmem184a	NM_144914	+ 1.40
Cystatin 9 precursor (Testatin)	Cst9	NM_009979	+ 1.35
Lactate dehydrogenase B	Ldhb	NM_008492	+ 1.34
Ras related proteinRab-12 (Rab-13)	Rab12	NM_024448	+ 1.34
Glutathione S-transferase Mu 1	Gstm1	NM_010358	+ 1.34
Junctional adhesion molecule 1 (JAM-A)	F11r	NM_172647	+ 1.33
Vinculin	Vcl	NM_009502	+ 1.31
Spectrin alpha 2 (fodrin)	Spnb2	NM_175836	+ 1.29
cysteine rich transmembrane BMP regulator 1 (chordin like)	Crim1	NM_015800	+ 1.28
Solute carrier family 2, facilitated glucose transporter, member 1 (Glut1)	Slc2a1	NM_011400	+ 1.27
Gata binding protein 1	Gata1	NM_008089	+ 1.26
Cathepsin a (PPCA)	Csta	NM_008906	+ 1.24
Protein kinase C, delta type	Prkcd	NM_011103	+ 1.24
Anti-Mullerian hormone type 2 receptor	Amhr2	NM_144547	+ 1.22
Rho GTPase-activating protein	Grit	NM_177379	+ 1.22
FSH receptor	Fshr	NM_013523	+ 1.19
Alpha actinin 4	Actn4	NM_021895	+ 1.17
Low density lipoprotein receptor-related protein 8 precursor	Lrp8	NM_001080926 / NM_053073	- 1.26
PHD finger protein 7	Phf7	NM_027949	- 1.42
Claudin11	Cldn11	NM_008770	- 2.13
Germ cell products			
Heat-shock protein beta-1	Hspb1	NM_013560	+ 1.98 / + 1.64
Calcium-regulated heat stable protein 1	Carhsp1	NM_025821	+ 1.52
zinc finger protein 1, Y linked	Zfy1	NM_009570	+ 1.31
FK506 binding protein 6	Fkbp6	NM_033571	+ 1.30
topoisomerase (DNA) II beta	Top2b	NM_009409	+ 1.28
Bcl2-interacting killer (Biklk)	Bik	NM_007546	+ 1.28
follistatin-like 3	Fstl3	NM_031380	+ 1.27
Ornithine decarboxylase antizyme	Oaz1	NM_008753	+ 1.27
structural maintenace of chromosomes 3 (Cspg6)	Smc3	NM_007790	+ 1.25
Protein kinase C, delta type	Prkcd	NM_011103	+ 1.24
G2/mitotic-specific cyclin B2	Ccnb2	NM_007630	- 1.20
Serine/threonin kinase 33	Stk33	XM_358897	- 1.22
TATA box binding protein-like protein 1	Tbpl1	NM_011603	- 1.23
Spermatogenesis associated glutamate (E)-rich protein 2	Speer2	NM_173069	- 1.24
LanC-like protein 1	Lancl1	NM_021295	- 1.26
Importin 13	Ipo13	NM_146152	- 1.26
	Ccdc89	XM_133591	- 1.29
Nephrocystin 1	Nphp1	NM_016902	- 1.30
ATP-dependant RNA helicase	Ddx25	NM_013932	- 1.30
Zona pellucida binding protein	Zpbp	NM_015785	- 1.30
Male-enhanced antigen-1	Mea1	NM_010787	- 1.30
Tektin 5	Tekt5	NM_001099275	- 1.30
Testis spermatocyte apoptosis related gene 6 protein	Dnajb113	NM_153527	- 1.33
Cell death regulator aven	Aven	NM_028844	- 1.33
Calcineurin B subunit isoform 2	Ppp3r2	NM_00100402	- 1.33
Cyclin A1	Ccna1	NM_007628	- 1.35
Thioredoxin domain containing 3	Txndc3	NM_181591	- 1.36
Actin-like-7-beta	Actl7b	NM_025271	- 1.36
Zona pellucida binding protein 2 isoform 1	Zpbp2	NM_027061	- 1.36
Testis specific gene A2	Tsga2	NM_025290	- 1.37
A disintegrin and metalloprotease domain 2	Adam2	NM_009618	- 1.37
A disintegrin and metalloprotease domain 5	Adam5	NM_007401	- 1.40
Asparagin-like 1	Asrgl1	NM_025610	- 1.40 / -1.39
DnaJ homolog subfamily B member 3	Dnajb3	NM_008299	- 1.41
Glutathione S-transferase Mu 5 (mGSTM5)	Gstm3	NM_010360	- 1.41
Mesoderm posterior 1	Mesp1	NM_008588	- 1.45
Four and a half LIM domain 4	Fhl4	NM_010214	- 1.46
Ring finger protein 36	Rnf36	NM_080510	- 1.46
Heat-shock protein beta-9	Hspb9	XM_905113	- 1.49
Meiosis expressed protein 1	Meig1	NM_008579	- 1.49

Cystein-rich secretory protein-2	Crisp2	NM_009420	- 1.50
Testis spermatocyte apoptosis-related gene 2	Spata4	NM_133711	- 1.52
Sperm associated antigen 17	Spag17	NM_028892	- 1.59
Cold shock domain protein A short isoform (Msy4)	Csda	NM_139117	- 1.62

815
816

Figure 1

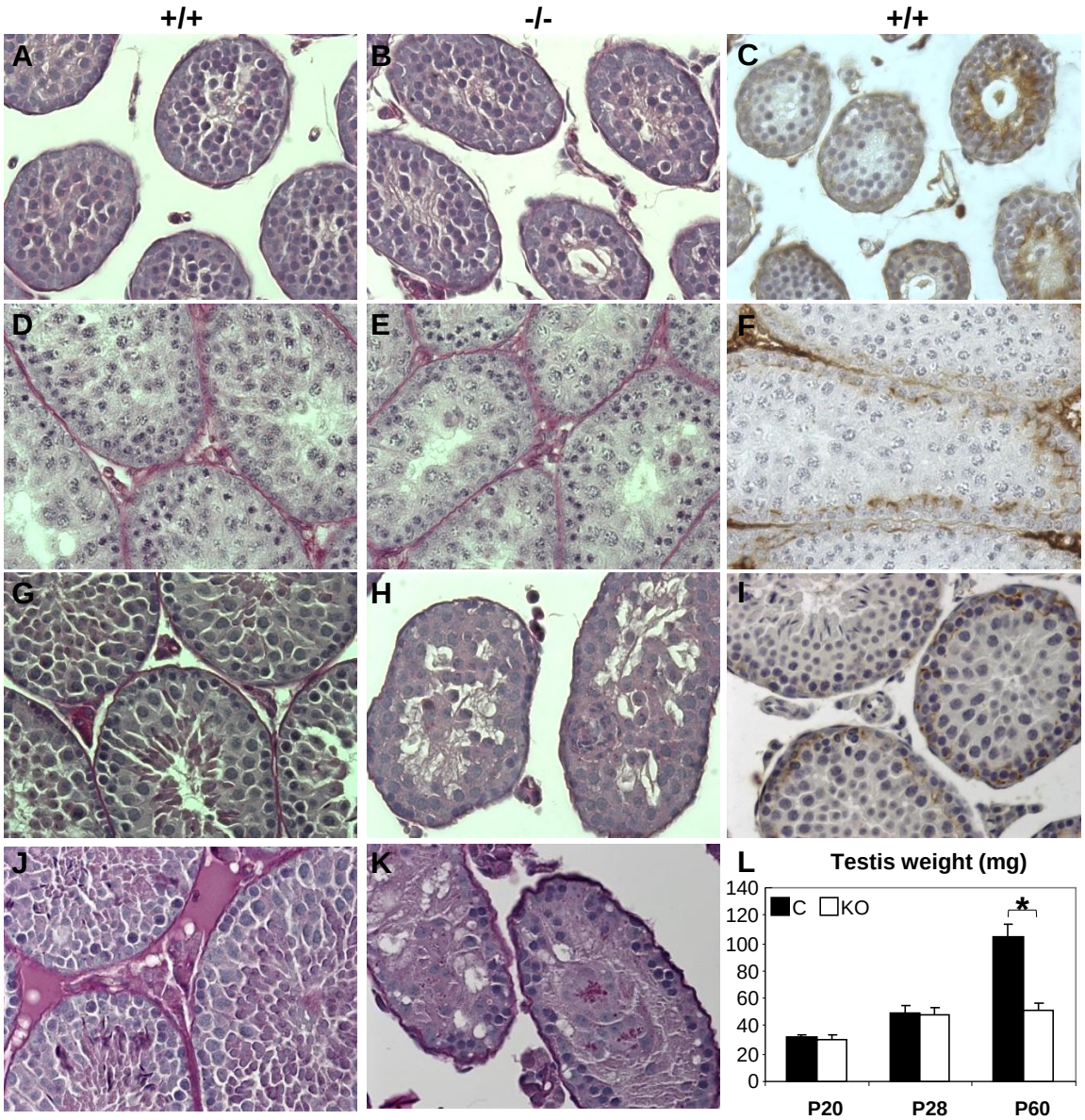

817
818

Figure 2

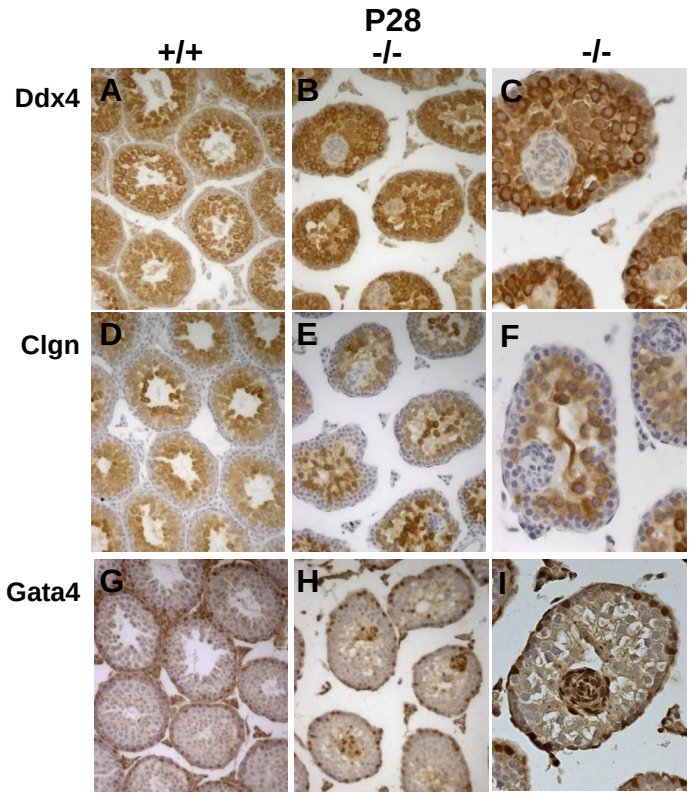

819
820

Figure 3

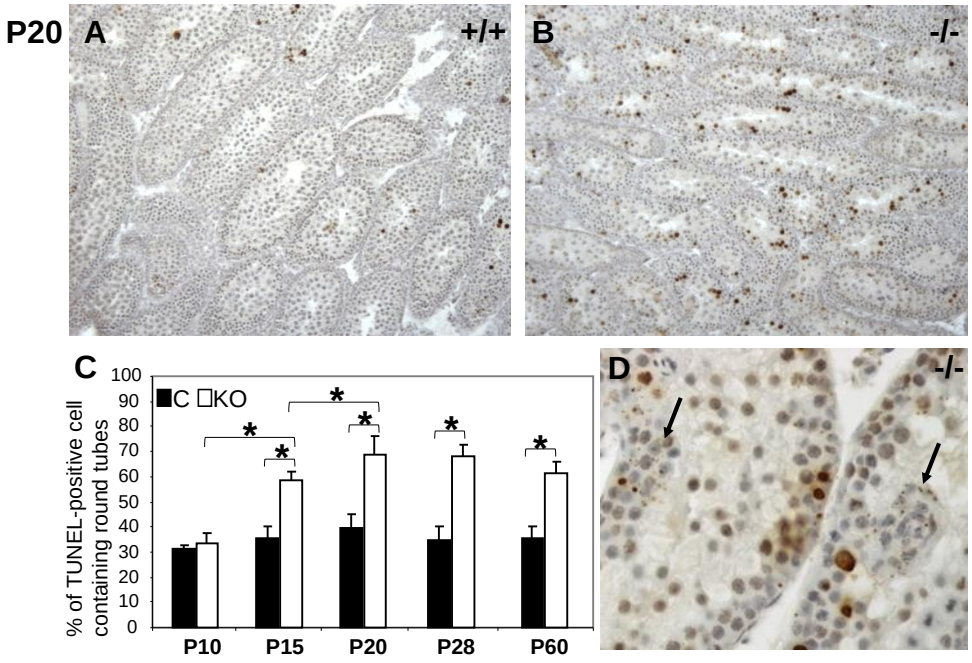

821
822

Figure 4

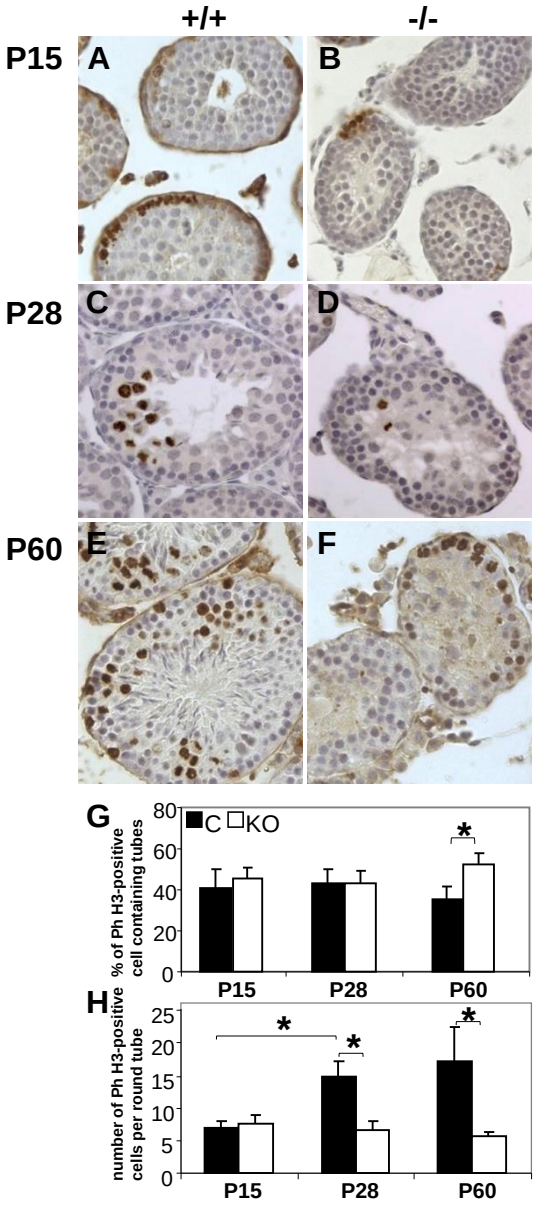

823
824

Figure 5

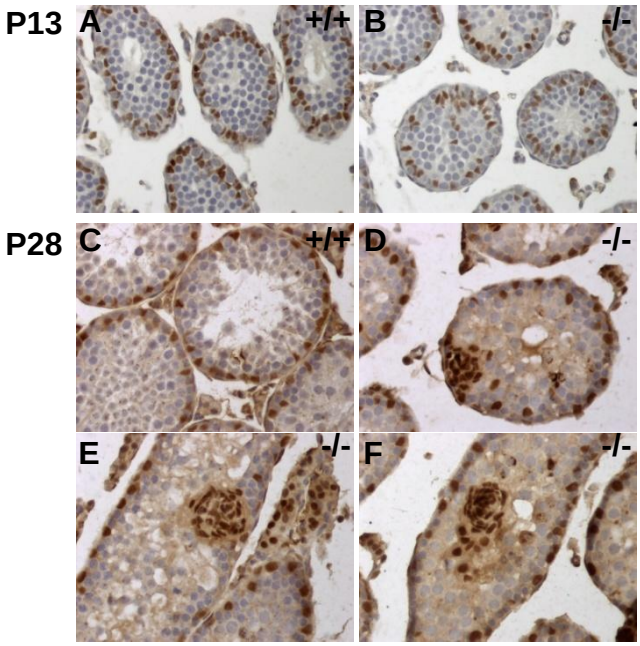

825
826

Figure 6

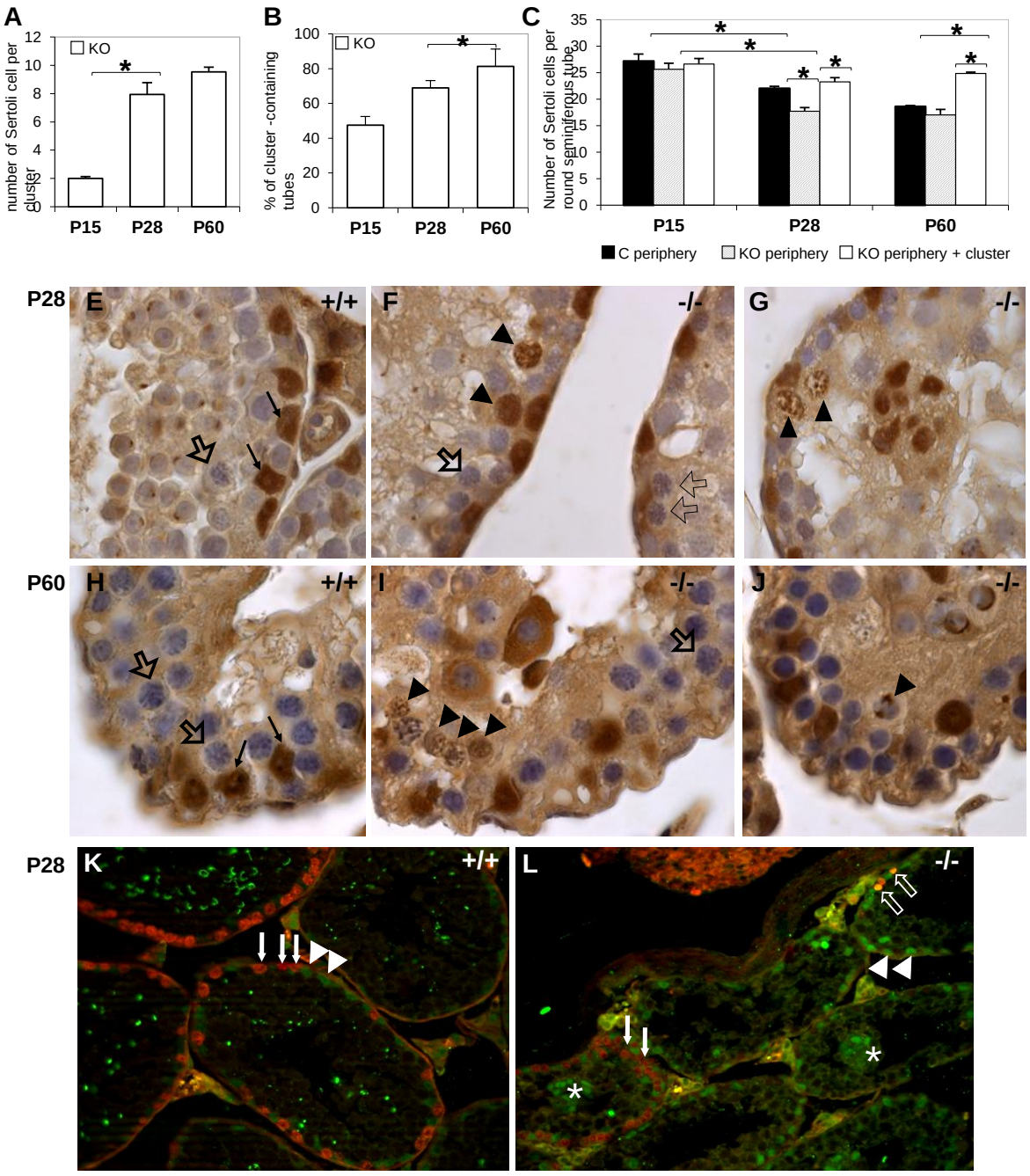

827
828

Figure 7

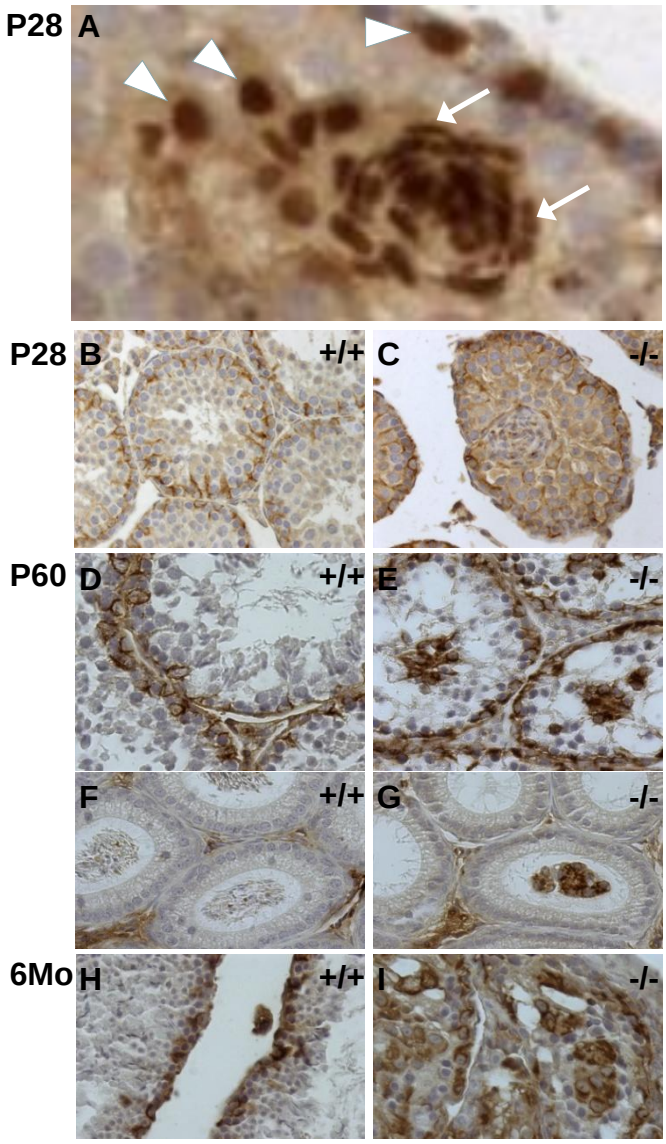

829